The Meteoritical Society

Meteoritics & Planetary Science 48, Nr 4, 628–640 (2013)
doi: 10.1111/maps.12076

Reclassification of Villalbeto de la Peña—Occurrence of a winonaite-related fragment in a hydrothermally metamorphosed polymict L-chondritic breccia

Addi BISCHOFF[1*], Kathryn A. DYL[2,3], Marian HORSTMANN[1], Karen ZIEGLER[3,4,5], Karl WIMMER[6], and Edward D. YOUNG[3,4]

[1]Institut für Planetologie, Wilhelm-Klemm-Str. 10, Münster 48149, Germany
[2]Department of Applied Geology, Curtin University of Technology, GPO U1987, Perth, Western Australia 6845, Australia
[3]Department of Earth and Space Sciences, UCLA, 3806 Geology, Los Angeles, California 90095, USA
[4]Institute of Geophysics and Planetary Physics, UCLA, 3845 Slichter Hall, Box 951567, Los Angeles, California 90095, USA
[5]Institute of Meteoritics, University of New Mexico, 221 Yale Blvd NE, 313 Northrop Hall, Albuquerque, New Mexico 87131, USA
[6]Rieskratermuseum Nördlingen, Eugene-Shoemaker-Platz 1, Nördlingen 86720, Germany
[*]Corresponding author. E-mail: bischoa@uni-muenster.de

(Received 25 May 2012; revision accepted 07 January 2013)

Abstract–The Villalbeto de la Peña meteorite that fell in 2004 in Spain was originally classified as a moderately shocked L6 ordinary chondrite. The recognition of fragments within the Villalbeto de la Peña meteorite clearly bears consequences for the previous classification of the rock. The oxygen isotope data clearly show that an exotic eye-catching, black, and plagioclase-(maskelynite)-rich clast is not of L chondrite heritage. Villalbeto de la Peña is, consequently, reclassified as a polymict chondritic breccia. The oxygen isotope data of the clast are more closely related to data for the winonaite Tierra Blanca and the anomalous silicate-bearing iron meteorite LEW 86211 than to the ordinary chondrite groups. The REE-pattern of the bulk inclusion indicates genetic similarities to those of differentiated rocks and their minerals (e.g., lunar anorthosites, eucritic, and winonaitic plagioclases) and points to an igneous origin. The An-content of the plagioclase within the inclusion is increasing from the fragment/host meteorite boundary (approximately An_{10}) toward the interior of the clast (approximately An_{52}). This is accompanied by a successive compositionally controlled transformation of plagioclase into maskelynite by shock. As found for plagioclase, compositions of individual spinels enclosed in plagioclase (maskelynite) also vary from the border toward the interior of the inclusion. In addition, huge variations in oxygen isotope composition were found correlating with distance into the object. The chemical and isotopical profiles observed in the fragment indicate postaccretionary metamorphism under the presence of a volatile phase.

INTRODUCTION

On January 4, 2004 an impressive daylight fireball was observed from Spain, Portugal, and the south of France at 16h46m45s UTC as a meteoroid penetrated into the Earth's atmosphere, generating shock waves that reached the ground and produced audible booms (Llorca et al. 2005). The first meteorite specimen was found on January 11, 2004, near the village of Villalbeto de la Peña, in northern Palencia (Spain). Until 2005 about 4.6 kg of meteorite mass had been recovered during several field campaigns (Llorca et al. 2005). The Villalbeto de la Peña meteorite has been classified as a moderately shocked (S4) L6 ordinary chondrite (Russell et al. 2004).

Llorca et al. (2005) described the fall circumstances and estimated the fireball energy released in the atmosphere from photometric, seismic, and infrasound data. They also summarized information on the meteorite recovery, strewn field geometry, meteorite petrology, chemical composition, and noble gas contents. The energy released from the impacting body

and cosmogenic radionuclide analysis allowed an estimate of the size of the meteoroid to 760 ± 150 kg (Llorca et al. 2005). In addition, Trigo-Rodríguez et al. (2006) discussed the atmospheric trajectory and heliocentric orbit of the meteoroid on the basis of detailed astrometric stellar calibrations of video and photographic records.

Based on refined dark flight calculations a new meteorite fragment with a mass of 526 g was recovered in 2005 within the mountain area of the strewn field. It is the second largest and 33rd listed stone out of 36 pieces making up a total mass of 5.2 kg. Parts of the surface are not covered by fusion crust, thus exposing an unusual dark fragment (Fig. 1). This new specimen of the Villalbeto de la Peña meteorite reveals that the rock is not a homogenous L6 chondrite, but a polymict breccia. Here, we report on the discovery of a black, plagioclase(-maskelynite)-rich clast having an oxygen isotopic composition, which is not related to ordinary chondrites. The mineralogical and chemical properties of the clast will be presented in detail and it will be argued why Villalbeto de la Peña has to be reclassified as a polymict ordinary chondrite breccia. Furthermore, we will discuss the origin and formation of the inclusion and implications for its evolution within the host rock. As will be shown, the meteorite must have been metamorphosed and shocked after the foreign fragment was incorporated into the Villalbeto de la Peña host rock. Preliminary data on this xenolithic clast and its hydrothermal metamorphic overprint have been published by Dyl et al. (2009). Detailed discussions on the time scales and conditions of aqueous activities have recently been presented separately by Dyl et al. (2012).

SAMPLES AND ANALYTICAL TECHNIQUES

Four aliquots from the hand specimen of Villalbeto de la Peña were separated: one of the black fragment (Fig. 1), one the host chondrite (both powders), and two fragments containing both black clast material and light host chondrite. These samples were used for mineralogical and oxygen isotopic analyses.

For the mineralogical studies of the black inclusion, a polished thick section containing both lithologies was studied by optical microscopy in reflected light and by electron microscopy. A JEOL 840A scanning electron microscope (SEM) was used to resolve the fine-grained material of the fragment, to identify mineral phases, and for energy dispersive (EDS) quantitative mineral analyses using the attached Pentafet detector (Oxford Instruments) and the INCA analytical program provided by Oxford Instruments.

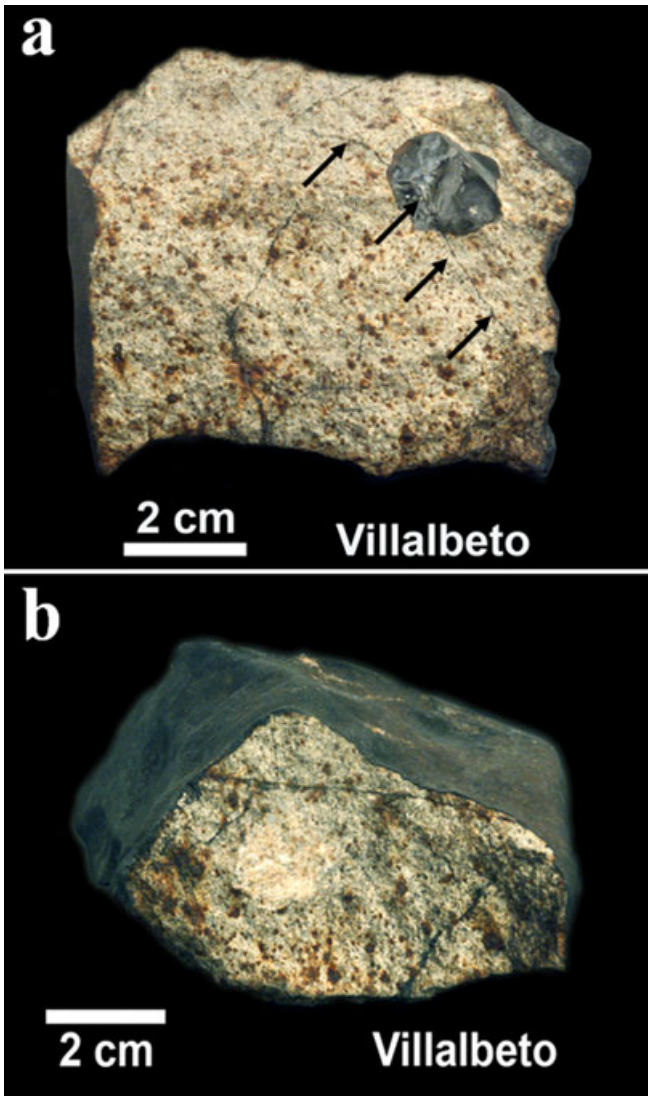

Fig. 1. Hand specimen of the Villalbeto de la Peña meteorite showing the brecciated character in the form of the centimeter-sized black (a) and light-colored (b) fragments. On the broken surface abundant shock veins are visible. A shock vein (arrows) is cutting through the black fragment (a) indicative of vein formation after the incorporation and annealing of the black fragment.

Most quantitative mineral analyses were obtained using a JEOL JXA 8900 electron microprobe (EMPA) operated at 15 keV and a probe current of 15 nA. Natural and synthetic standards of well-known compositions were used as standards for wavelength dispersive spectrometry. These are jadeite (Na), sanidine (K), diopside (Ca), disthen (Al), fayalite (Fe), chromite (Cr), pentlandite (Ni), hypersthene (Si), San Carlos olivine (Mg), rhodonite (Mn), rutile (Ti), tugtupite (Cl), and willemite (Zn). The matrix corrections were made according to the $\Phi\rho(z)$ procedure of Armstrong (1991).

Raman Spectroscopy

Qualitative Raman spectra of the feldspathic material both in the host rock and the inclusion were obtained with a Horiba XploRA Raman spectrometer equipped with a He-Ne laser as excitation source. Using the 638 nm line of the laser the scattered Raman light was collected with a 100× objective equipped with a charge-coupled device detector in the range of 100–1000 cm^{-1} after being dispersed via a grating (1800 grooves mm^{-1}). The slit width of the spectrometer was set to 100 μm, the confocal hole to 500 μm. Each spot was analyzed with three repetitions of 60 s each and the gained intensities of each repetition were averaged for the final spectrum. Any possible spectrometer drift was monitored by measurements of the 520.7 cm^{-1} line of silicon. Two of the gained spectra indicate contamination from surrounding Cr-spinel.

Oxygen Isotope Analyses

For bulk O-isotopic analyses, the meteorite samples were gently disintegrated with a mortar and pestle. Pieces of the crushed samples with masses of 1–1.5 mg were picked for O-isotopic analyses. High-precision oxygen isotope analyses were made using a 20W CO_2 laser attached to a laser-fluorination (F_2-gas) vacuum extraction line (Sharp 1990).

A fragment containing both host and clast material from Villalbeto de la Peña was measured via ultraviolet (UV) laser ablation fluorination to investigate the possible presence and degree of an oxygen isotopic gradient across the clast and the L6 ordinary chondrite host. Complete descriptions of the performed O-isotope analysis techniques are given in Young et al. (1998) and Dyl et al. (2012).

LA-ICP-MS

Trace element concentrations were determined on a polished thick section by laser ablation-inductively coupled plasma-mass spectrometry (LA-ICP-MS) at the Institut für Mineralogie, Münster, using a ThermoFisher Element single collector ICP-MS coupled to a laser ablation system with an output wavelength of 193 nm. The polished section was ablated in a 150 mm Large Format Cell. The laser was operated with a uniform energy density of approximately 4 J cm^{-2} and a 5 Hz repetition rate. The blank was measured for 20 s, the peak for 40 s, and wash-out was attuned to 15 s. The spot size was set to 45 μm and laser measurements were performed on the same spots for which EPMA data were collected before with a defocused beam for internal standardization. The international standard reference materials NIST SRM-612 and BIR1-G were used: NIST SRM-612 as an external standard and BIR1-G for additional verification of the precision and accuracy of the analyses. The following elements were monitored in low resolution mode: ^{29}Si, ^{43}Ca, ^{45}Sc, ^{47}Ti, ^{51}V, ^{66}Zn, ^{69}Ga, ^{75}As, ^{85}Rb, ^{89}Y, ^{90}Zr, ^{93}Nb, ^{95}Mo, ^{137}Ba, ^{139}La, ^{140}Ce, ^{141}Pr, ^{146}Nd, ^{147}Sm, ^{153}Eu, ^{157}Gd, ^{159}Tb, ^{163}Dy, ^{165}Ho, ^{166}Er, ^{169}Tm, ^{172}Yb, ^{175}Lu, ^{178}Hf, ^{181}Ta, ^{182}W, ^{185}Re, ^{195}Pt, ^{232}Th, and ^{238}U. Data were processed with the Glitter data reduction software provided by the ARC National Key Centre for Geochemical Evolution and Metallogeny of Continents (GEMOC) and CSIRO Exploration and Mining using Si as internal standard. Measurements covered the three mineralogically different portions of the dark inclusion and the number of analyses performed on each domain corresponds to its modal abundance in the studied thin section. By calculating the average of the analyses, the weighted average concentration for each element was obtained. In those cases where concentrations were below the detection limit for a single analysis, the detection limit was used for the calculation of the average instead. Concentrations listed in the GeoReM database for the reference material BIR1-G were reproduced within the 2 sigma standard error of the concentrations obtained for BIR1-G in the runs here.

RESULTS

Original Classification

The Villalbeto de la Peña meteorite has been classified as a moderately shocked (S4) L6 ordinary chondrite (Russell et al. 2004; Llorca et al. 2005). Based on these studies the bulk density of the Villalbeto de la Peña meteorite is 3.42 g cm^{-3}, which is within the 3.40 ± 0.15 g cm^{-3} range for L6 chondrites (Wilkinson and Robinson 2000). Numerous shock veins were detected in the bulk rock, which contains <2–3 vol% metallic Fe-Ni, occurring as kamacite (6.9 ± 0.5 wt% Ni, 1.0 ± 0.1 wt% Co), taenite (37.6 ± 1.9 wt% Ni, 0.30 ± 0.05 wt% Co), and plessite (Llorca et al. 2005). The composition of troilite is very homogeneous (63.3 ± 0.2 wt% Fe, 36.7 ± 0.2 wt% S) and the olivine ($Fa_{24.2 \pm 0.2}$ mol%) and low-Ca pyroxene ($Fs_{20.3 \pm 0.2}$, $Wo_{1.6 \pm 0.2}$ mol%; Llorca et al. 2005) are in the range of L-group chondrites ($Fa_{23.0–25.8}$, $Fs_{18.7–22.6}$; Gomes and Keil 1980; Rubin 1990). The homogeneity of olivine and pyroxene compositions, the occurrence of 50 μm-size plagioclase grains, and the recrystallized texture led Llorca et al. (2005) to classify the Villalbeto de la Peña meteorite as a type 6 chondrite. Based on the occurrence of weak mosaicism and sets of planar

fractures in the olivine grains a shock stage S4 was determined using the classification scheme of Stöffler et al. (1991). Llorca et al. (2005) mentioned that plagioclase in Villalbeto de la Peña ($Ab_{69.2}Or_{7.3}$) differs significantly from the mean composition in equilibrated L chondrites ($Ab_{84.2}Or_{5.6}$; van Schmus and Ribbe 1968).

The Brecciated Nature of the Villalbeto de la Peña Meteorite

A black- and a light-colored fragment were detected on the broken surface (Fig. 1) of the new Villalbeto de la Peña fragment recovered in 2005 clearly pointing to a brecciated nature of the meteorite. Although Llorca et al. (2005) described a recrystallized porphyritic olivine chondrule fragment, the occurrence of large, centimeter-sized lithic fragments has not been reported. The black fragment has an optically featureless, homogeneous appearance in hand specimen and forms a sharp contact with the host chondrite. Shock veins visible in the bulk rock also cut through the black clast (Fig. 1a) indicating that the shock event occurred after incorporation of the fragment and lithification of the bulk breccia. The rock does not have the typical light/dark structure as observed for many chondrite regolith breccias. Other occurrences of this type of black clasts in other specimens are unknown.

Mineralogy and Mineral Chemistry of the Black Fragment

The black, plagioclase-rich clast contains numerous very fine-grained inclusions of metal, sulfide, and Cr-spinel embedded in an amorphous, stoichiometric plagioclase matrix and is about 2 cm in apparent diameter (Figs. 1 and 2). The sample studied also contains some host material (Figs. 2a and 2c) and allows study of the transition between the host L6-rock and the fragment. As noted by Llorca et al. (2005) olivine in the host rock shows weak mosaicism, which indicates a shock stage of S4 (Stöffler et al. 1991). Ordinary chondrites of shock stage S4 can contain significant amounts of isotropic plagioclase (maskelynite; Stöffler et al. 1991); in addition Stöffler et al. (1986) could show that the degree of partial or total isotropization of plagioclase is a function of the An-content. At a shock pressure of 30 GPa complete transformation of plagioclase into maskelynite is reached for plagioclase with approximately $An_{>50}$, whereas plagioclase with approximately An_{20} is still completely crystalline (Stöffler et al. 1986; Bischoff and Stöffler 1992). Exactly this chemically controlled transformation is observed in Villalbeto de la Peña. Raman spectra of the An-poor plagioclase in the host and close to the boundary within the black fragment reveal that it is still crystalline (Fig. 3). With increasing distance from the contact, the Raman spectra of plagioclase indicate an increasing transformation

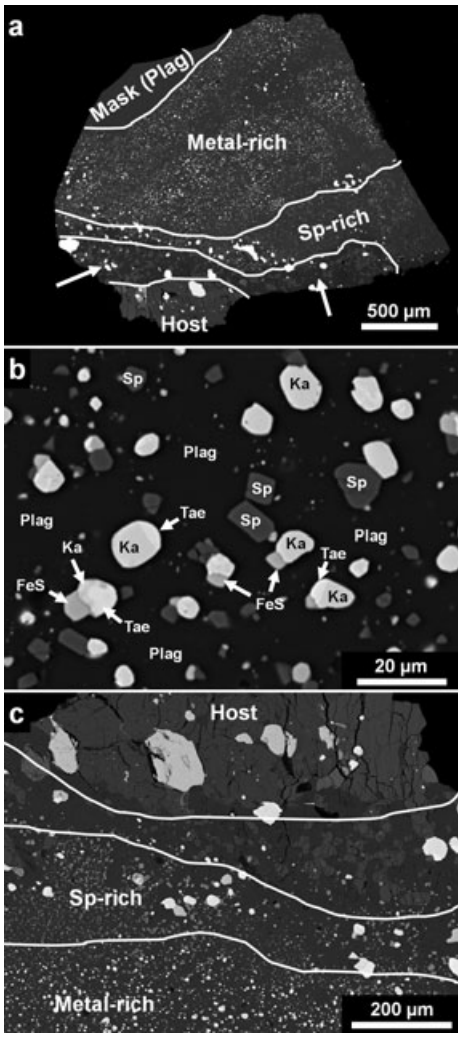

Fig. 2. a) Overview of the studied thin section of the Villalbeto de la Peña meteorite. The different portions that were identified are outlined. Starting with the host rock (Host), this domain is followed by a transition zone with host rock grains in plagioclase matrix (arrows). Please note that most plagioclase in the interior of the metal-rich zone has been transformed into maskelynite by shock. The outer portion of the black fragment is dominated by spinel inclusions in plagioclase and low metal abundance (Sp-rich) and followed by the dominating portion with abundant, mainly small metal grains (Metal-rich). In the upper left of the inclusion plagioclase (maskelynite) occurs. b) Typical area from the interior of the fine-grained, black fragment. Cr-spinels (Sp), metals (kamacite [Ka], taenite [Tae]), and sulfides (FeS) are embedded in a plagioclase-groundmass (Plag). c) Transition between the host chondrite and the black clast. Note that within the first approximately 300 µm of the fragment abundant spinels (light gray) and less metal (white) occur. Backscattered electron images.

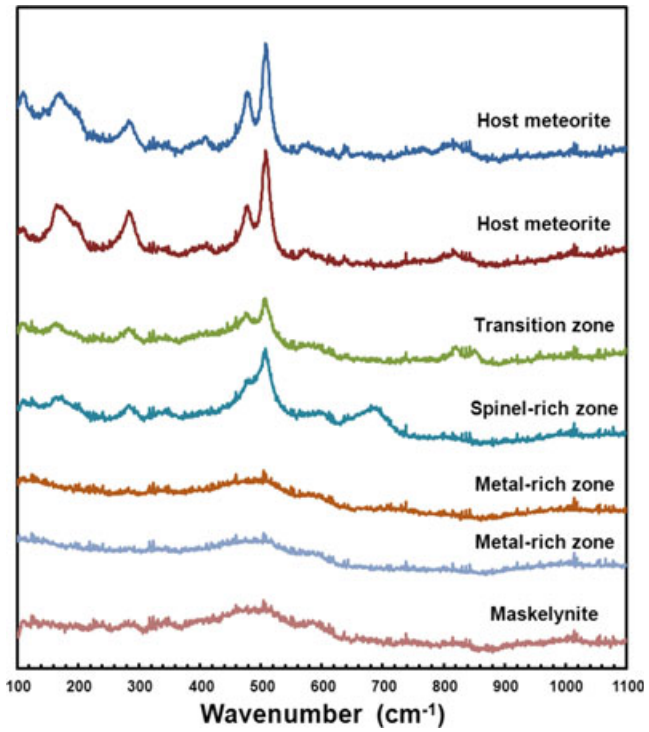

Fig. 3. Raman spectra documenting the plagioclase-maskelynite transition starting in the host meteorite (top) merging into the fragment ending at pure maskelynite (bottom). The characteristic Raman features of plagioclase observed in the host meteorite fade away with increasing distance from the host rock boundary and are already gone in the metal-rich zone. Spectra intensities are given in arbitrary units on the *y*-axis.

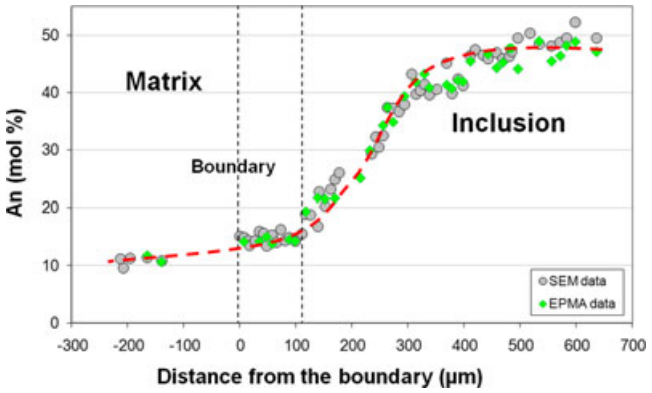

Fig. 4. Chemical profile illustrating the increase in An-component of plagioclase (maskelynite). The An-content of plagioclase is continuously increasing from the host (approximately An_{10}) toward the center of the black clast ($An_{50–52}$).

(isotropization) of the mineral. Along with increasing An-content, the plagioclase in the fragment is successively transformed into maskelynite, which is documented by a degradation of the typical plagioclase features in the range of approximately 470–510 cm^{-1}. Thus, this sample can be used to determine the shock pressure the bulk rock has seen: approximately 30 GPa. This shock event certainly occurred as a late stage process after metamorphism, perhaps also causing the shock vein formation in the bulk rock (Fig. 1) and/or the ejection of the rock from the parent body. In the following we will continue to refer to "plagioclase" although it will be (at least partially) "maskelynite" in most cases.

Compositionally, the bulk fragment is rich in Ca, Na, and Al. Defocused-beam microprobe analyses (30 single spots with 50 µm spot size including the metal-rich, spinel-rich, and plagioclase-rich areas in roughly balanced proportions as shown in Fig. 2a) of the main oxides within the bulk inclusion revealed an average of approximately 8.5 wt% CaO, 6 wt% Na_2O, 26 wt% Al_2O_3, 50 wt% SiO_2, 6.5 wt% FeO (all Fe as FeO), and 2 wt% Cr_2O_3. The MgO-concentration of the bulk fragment of about 0.5 wt% is remarkably low. The dominating mineral phase is plagioclase, which constitutes the groundmass (Fig. 2b) of the inclusion. The composition of plagioclase is variable, ranging from approximately An_{12} to An_{52}. The typical plagioclase from metamorphosed ordinary chondrites has about 10–12 mol% An. Similar values for plagioclase were found in the host rock of Villalbeto de la Peña close to the black fragment. However, in the center of the fragment, the composition of plagioclase reaches approximately $An_{49–52}$. We have obtained an An-profile starting 200 µm within the host chondrite and ending about 700 µm within the black clast (Fig. 4; Table 1). The profile illustrates that the An-contents of plagioclase continuously increase from the surrounding host rock (approximately An_{10}) toward the center of the black fragment where the maximum (approximately $An_{49–52}$) is reached about 500 µm away from the boundary between these two lithologies.

Metal, troilite, and Cr-spinel have been detected as inclusions within the plagioclase (Fig. 2c) and appear heterogeneously dispersed. In general, these phases are smaller than 20 µm. A total of three different domains within the inclusion (Fig. 2a) were defined. (i) Within the first approximately 300 µm of the fragment abundant spinel and fewer metal grains occur (Fig. 2c). (ii) The metal abundances increase toward the interior of the inclusion and the mostly rounded grains typically consist of an intergrowth of kamacite and taenite (Fig. 2b). (iii) In the interior of the black fragment nearly pure plagioclase (up to about 500 µm in apparent size, Fig. 2a) was found (approximately An_{51}). It is unclear how this plagioclase is related to domain (ii); only minor amounts of spinel, metal, and

Table 1. Variation of plagioclase (maskelynite) compositions from the host (1) into the center of the fragment (9). Rare, more calcic plagioclase up to An_{52} was detected by SEM-EDS (see Fig. 4).

No.	Na_2O	MgO	Al_2O_3	SiO_2	K_2O	CaO	FeO	Total	An	Or
1	10.1	n.d.	21.2	66.5	1.07	2.31	0.64	101.82	9.9	5.8
2	8.9	n.d.	21.7	65.2	0.98	2.85	0.58	100.21	11.7	5.7
3	8.4	0.05	22.6	62.6	0.68	4.4	0.47	99.20	21.5	3.9
4	7.2	n.d.	25.8	58.7	0.75	7.4	0.62	100.47	34.9	4.8
5	6.4	n.d.	26.3	58.4	0.51	7.9	0.35	99.86	39.4	3.0
6	6.2	0.10	27.8	55.9	0.38	9.7	0.46	100.54	45.5	2.1
7	6.0	0.06	27.8	55.9	0.47	10.1	0.55	100.88	46.7	2.6
8	5.9	n.d.	28.1	55.7	0.41	10.2	0.47	100.78	47.3	2.3
9	5.8	n.d.	28.9	55.3	0.29	10.4	0.44	101.13	48.9	1.6

EPMA data in wt%; n.d. = not detected; An- and Or-contents in mol%. The detection limit for MgO is below 0.04 wt%.

Table 2. Spinel compositions from the host (1) toward the center of the inclusion (11). The mean composition for spinel from the bulk rock given by Llorca et al. (2005) is given for comparison.

No.	Al_2O_3	Cr_2O_3	MgO	SiO_2	CaO	MnO	TiO_2	FeO	Total
Llorca	5.9	57.0	2.6	0.04	0.04	0.82	2.9	30.8	100.10
1	6.1	53.5	2.7	0.09	0.04	0.68	2.5	32.0	97.61
2	9.9	52.2	4.3	0.05	0.06	0.56	3.2	30.3	100.57
3	12.6	49.3	5.1	0.05	0.21	0.71	2.5	28.3	98.77
4	20.6	44.7	6.7	n.d.	0.16	0.56	1.28	25.9	99.90
5	22.7	42.9	7.0	0.06	0.08	0.42	1.05	25.6	99.81
6	29.1	37.5	8.1	0.08	0.16	0.51	0.70	24.6	100.75
7	33.7	32.9	9.1	0.11	0.28	0.42	0.38	23.8	100.69
8	38.1	29.3	10.3	0.07	0.21	0.57	0.07	22.1	100.72
9	39.2	27.4	10.9	0.08	0.17	0.50	0.13	21.9	100.28
10	42.1	25.9	11.3	0.16	0.22	0.28	n.d.	21.3	101.26
11	42.9	25.4	11.0	0.05	0.21	0.44	0.09	21.5	101.59

n.d. = not detected; detection limits for SiO_2 and CaO are below 0.04 wt% and for TiO_2 below 0.07 wt%; all Fe as FeO; electron microprobe data.

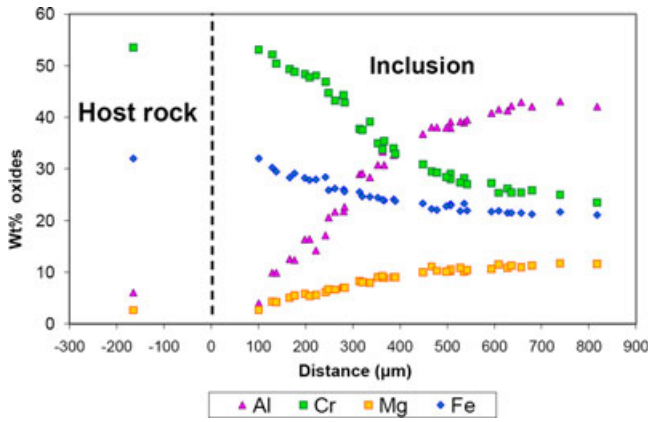

Fig. 5. Variation of spinel compositions from the host meteorite toward the center of the black fragment (compare Table 2).

sulfide inclusions occur at the contact. Limited analyses revealed that kamacite and taenite have 5–7 wt% Ni and up to 42 wt% Ni, respectively. The Cr-content of spinel is increasing toward the fragment/host rock boundary (Fig. 5). At the boundary (zone I), the Cr-spinels have approximately 52 wt% Cr_2O_3, 30 wt% FeO, 4 wt% MgO, 1 wt% MnO, 10 wt% Al_2O_3, and 3 wt% TiO_2. Thus, these Cr-spinels are more similar in composition to Cr-spinels in the host rock of the Villalbeto de la Peña chondrite (Cr_2O_3: 57 wt%, FeO: 30 wt%, Al_2O_3: 6 wt%; Llorca et al. 2005; Table 2) than to those toward the center of the black clast (zone II) or to those in other spinel-bearing objects of ordinary chondrites (e.g., Al-rich chondrules and CAIs; e.g., Bischoff and Keil 1983, 1984; Bischoff et al. 1989). The Cr-bearing spinels in the center of the fragment have a relatively high Al_2O_3 composition (Cr_2O_3: 25–28 wt%, FeO: 20–22 wt%, MgO: 10–12 wt%, Al_2O_3: 38–43 wt%; Table 2). Pyroxene and olivine were not detected within the black fragment. Considering the zones which are rich in metal or spinel (+plagioclase; Fig. 2a) the reason for the variation in mineralogy (plag + metal versus plag + spinel) is unclear.

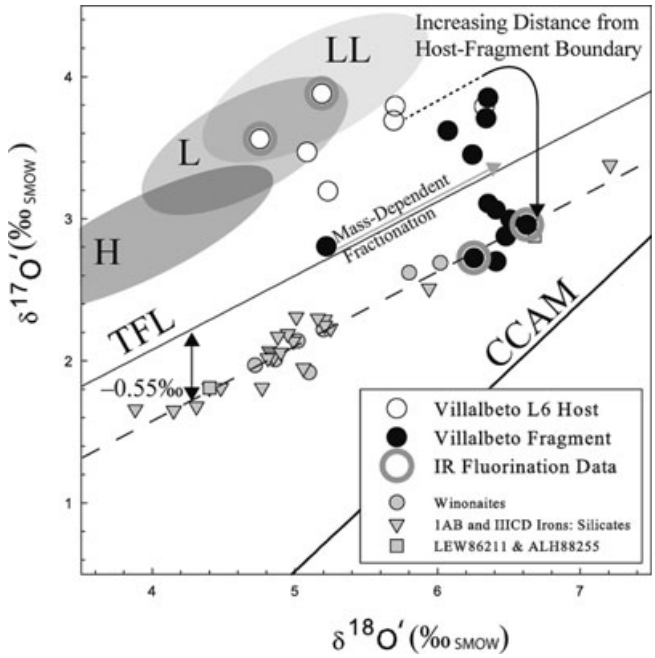

Fig. 6. Oxygen isotopic composition of Villalbeto de la Peña and fragment in 3-isotope space. Fluorination analyses of host material are white circles; fragment material is indicated with black circles. Analyses encircled in dark gray are CO_2 laser-fluorination analyses; all other data points are in situ UV laser ablation-fluorination analyses. One data point exhibits mass-dependent fractionation during analysis (e.g., adsorption of $O_{2(g)}$ to fluorination products, incomplete freezing of $O_{2(g)}$ to Si-gel gas during analysis) and is indicated as such. The small volume of gas measured confirms this effect, which does not impact $\Delta^{17}O$. Gray ellipses illustrate where H, L, and LL ordinary chondrites plot. Other meteoritic materials exhibiting similar $\Delta^{17}O$ are plotted for comparison (Clayton et al. 1991). The solid line is the terrestrial mass fractionation line. The bold line represents the CCAM line. A dashed line with slope = 0.52 corresponds to a $\Delta^{17}O'$ of −0.55‰. The (′) indicates "linearized delta."

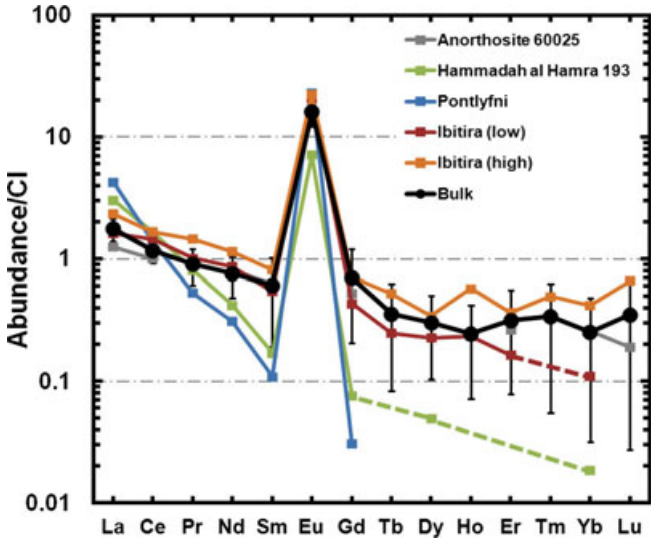

Fig. 7. REE-patterns of the black Villalbeto de la Peña bulk rock clast (black dots; 1σ-error; compare Table 3) in comparison with the lunar anorthosite 60025 (Wiesmann and Hubbard 1975), and plagioclase from the anomalous eucrite Ibitira (Hsu and Crozaz 1996) and from the winonaites Pontyfli and Hammadah al Hamra 193 (Floss et al. 2007, 2008).

At the boundary between the host rock and the clast, an approximately 100 μm wide transition zone is observed in which coarse olivine is enclosed within plagioclase (Fig. 2c).

Oxygen Isotopes

The Villalbeto de la Peña host meteorite has a $\Delta^{17}O'$; value of ≈1.1‰ ($\delta^{17}O'$; = 3.7‰; $\delta^{18}O'$; = 5.0‰; Fig. 6), grouping it with L/LL ordinary chondrites (Clayton et al. 1991). In contrast, the $\Delta^{17}O'$; value of interior samples of the black fragment is −0.56‰ ($\delta^{17}O$ = 2.8‰; $\delta^{18}O$ = 6.4‰), and therefore dramatically deviates from ordinary chondrites (Fig. 6). The result confirms that the fragment is unrelated to the bulk meteorite. The data are more closely related to those for the winonaite Tierra Blanca ($\delta^{17}O$ = 2.69‰, $\delta^{18}O$ = 6.02‰) and the anomalous silicate-bearing iron meteorite LEW 86211 ($\delta^{17}O$ = 2.88‰, $\delta^{18}O$ = 6.68‰) than to the ordinary chondrite groups (Clayton et al. 1991; Clayton and Mayeda 1996). In the clast a clear decrease in $\Delta^{17}O'$; as a function of distance from the host is observed as clearly shown in fig. 2 of Dyl et al. (2009). The gradient in $\Delta^{17}O'$; extends 1000–1500 μm into the clast. These oxygen data are discussed in more detail by Dyl et al. (2012).

Trace Elements

The average (bulk) concentrations of 30 laser measurements are given in Table 3 and the bulk rare earth element pattern normalized to CI-chondritic abundance (Anders and Grevesse 1989) is shown in Fig. 7. The bulk composition listed in Table 3 is a mixture of the inclusion-poor, plagioclase-rich area (five analyses), spinel-rich areas close to the host/inclusion boundary (eight analyses), and 17 analyses of the interior with abundant metal. The number of analyses in each domain roughly corresponds to its modal abundance in the studied thin section. The REE-pattern (Fig. 7) shows a distinct positive Eu-anomaly (Eu* = approximately 25, calculated as $Eu^* = Eu_N/\sqrt{(Sm_N \times Gd_N)}$ using the CI-normalized values) and a slight decrease from the LREE (e.g., La approximately 1.7 × CI) to the HREE (Tb-Lu: <0.5 × CI). The data for the HREE are close to or at the detection limits.

Table 3. Minor and trace element concentrations of the black inclusion. The bulk composition is a mixture of inclusion-poor, plagioclase-rich area (5 analyses), spinel-rich areas close to the host/inclusion boundary (8 analyses), and 17 analyses of the typical, mineralogically dominating interior.

Data	Sc	2σ	Ti	2σ	V	2σ	Zn	2σ	Ga	2σ	As	2σ	Rb	2σ	Y	2σ	Zr	2σ	Nb	2σ	Mo	2σ
Inclusion-free (5)	0.57	0.42	321	70	0.25	0.18	2.04	1.48	11.0	1.7	0.80	0.59	2.7	0.6	0.43	0.11	1.0	0.7	0.18	0.06	0.15	0.11
Sp-rich 300 μm (8)	1.10	0.52	836	187	112	19	289	50	27.6	4.4	0.95	0.68	4.2	1.0	0.11	0.06	3.5	1.1	1.34	0.33	0.26	0.16
Interior (17)	1.08	0.47	593	142	8.6	1.6	124	23	20.8	3.5	0.88	0.59	3.3	0.8	0.24	0.07	1.4	0.8	0.45	0.13	0.29	0.18
Bulk (30)	1.00	0.48	613	142	34.7	6.0	147.6	27	21.0	3.4	0.88	0.61	3.4	0.8	0.23	0.07	1.9	0.9	0.65	0.17	0.26	0.16

	Ba	2σ	La	2σ	Ce	2σ	Pr	2σ	Nd	2σ	Sm	2σ	Eu	2σ	Gd	2σ	Tb	2σ	Dy	2σ	Ho	2σ
Inclusion-free (5)	17.5	3.3	0.42	0.07	0.81	0.14	0.10	0.03	0.48	0.14	0.14	0.07	1.04	0.22	0.13	0.09	0.02	0.01	0.13	0.06	0.02	0.01
Sp-rich 300 μm (8)	17.5	3.4	0.46	0.08	0.65	0.12	0.07	0.02	0.25	0.11	0.07	0.06	0.86	0.19	0.15	0.11	0.01	0.01	0.06	0.04	0.01	0.01
Interior (17)	15.8	3.3	0.39	0.07	0.70	0.14	0.08	0.02	0.35	0.12	0.08	0.06	0.89	0.21	0.14	0.10	0.01	0.01	0.07	0.05	0.01	0.01
Bulk (30)	16.5	3.3	0.41	0.07	0.71	0.13	0.08	0.02	0.34	0.12	0.09	0.06	0.91	0.20	0.14	0.10	0.01	0.01	0.07	0.05	0.01	0.01

	Er	2σ	Tm	2σ	Yb	2σ	Lu	2σ	Hf	2σ	Ta	2σ	W	2σ	Re	2σ	Pt	2σ	Th	2σ	U	2σ
Inclusion-free (5)	0.04	0.03	0.011	0.009	0.04	0.03	0.011	0.008	0.04	0.03	0.02	0.01	0.03	0.03	0.006	0.011	0.09	0.06	0.003	0.004	0.001	0.001
Sp-rich 300 μm (8)	0.05	0.04	0.008	0.007	0.04	0.03	0.008	0.008	0.08	0.05	0.13	0.04	0.05	0.03	0.013	0.011	0.12	0.08	0.010	0.007	0.003	0.002
Interior (17)	0.05	0.04	0.008	0.006	0.04	0.04	0.008	0.008	0.05	0.03	0.03	0.02	0.05	0.04	0.014	0.011	0.13	0.08	0.009	0.006	0.002	0.001
Bulk (30)	0.05	0.04	0.008	0.007	0.04	0.04	0.008	0.008	0.05	0.04	0.05	0.02	0.05	0.03	0.013	0.011	0.12	0.08	0.008	0.006	0.002	0.001

Average data (ppm) were calculated as the weighted mean of the single values. In the case of concentrations being below detection limit, the detection limit was used for calculation of the average instead. 2σ = 2σ standard error.

The REE-patterns for all three analyzed areas (not shown) are similar and seemingly dominated by a characteristic plagioclase pattern with the strong positive Eu-anomaly (compare Table 3). Considering other minor and trace elements, especially the V and Zn concentrations show significant variation. Due to abundant spinel close to the host/inclusion boundary, Zn and V are more than 100 times higher in abundance in the spinel-rich area than within the plagioclase-rich area. The refractory siderophile elements (e.g., W, Re, Mo, Pt) are all depleted up to approximately 1 order of magnitude compared with the CI abundances (Anders and Grevesse 1989).

DISCUSSION

Reclassification of Villalbeto de la Peña

The recognition of fragments within the Villalbeto de la Peña meteorite clearly bears some consequences for the classification of the rock. The meteorite was originally classified as an unbrecciated L6 rock by Llorca et al. (2005). Their thin section description did not indicate the brecciated nature of the bulk rock. Although Llorca et al. (2005) described a recrystallized PO chondrule fragment, the occurrence of large centimeter-sized lithic fragments has not been reported. The findings described here clearly indicate that Villalbeto de la Peña is a breccia. Since the oxygen isotope data clearly show that the black clast is not of L chondrite heritage (Fig. 6), we further have to follow that the bulk rock is polymict. Consequently, Villalbeto de la Peña has to be reclassified as a polymict chondritic breccia.

Foreign Fragments within Ordinary Chondrite Breccias

The occurrence and abundance of foreign clasts in meteorites gives a good measure of the degree of mixing among asteroids and the relative abundance of different types of material at different times and places in the asteroid belt. Excellent examples to study the processes of accretion, metamorphism, differentiation, brecciation, and reaccretion in one meteorite are the polymict breccias Almahata Sitta and Kaidun (e.g., Zolensky and Ivanov 2003; Bischoff et al. 2010; Horstmann et al. 2012). Dark or black inclusions (clasts) in chondrites have been found in many chondrites (e.g., Fruland et al. 1978; Bischoff et al. 1988, 2006, 2011; Brearley et al. 1991; Endreß et al. 1994; Rubin and Bottke 2009). The latter authors described CM-like clasts in H-group ordinary chondrites. Similarities exist between the Villalbeto black inclusion and the Cr-rich chondrules and inclusion found in the other ordinary chondrites (e.g., Bischoff and Keil 1983, 1984; Brearley et al. 1991; Krot et al. 1993). Brearley et al. (1991) describe a Cr-rich inclusion within the Los Martinez (L6) chondrite breccia, which has distinct mineralogical similarities to the inclusion described here. Both samples are plagioclase-rich and have abundant Cr-rich spinel. Based on the bulk compositional zoning, Brearley et al. (1991) suggested that the inclusion in Los Martinez formed by "fractional crystallization from a melt, which may have formed as a liquid condensate or by melting of solid condensates, in the solar nebula." Unfortunately, no oxygen isotope data for this fragment exist to allow more detailed suggestions on its origin and evolution.

Considering ordinary chondrites, the occurrence of clasts from different ordinary chondrites groups in a specific host chondrite breccia is relatively rare (Bischoff et al. 2006). Within the St. Mesmin LL chondrite, intensely shocked H-group chondrite fragments were encountered (Dodd 1974). An LL5 clast was found in the Dimmitt H-chondrite regolith breccia (Rubin et al. 1983), and an L-group melt rock fragment was described in the LL chondrite Paragould (Fodor and Keil 1978). Similarly, olivines inside distinct fragments in Adzhi-Bogdo (LL3-6) clearly fall in the range of L-group chondrites (Bischoff et al. 1993, 1996, 2006). An LL-chondritic xenolith was observed within the Tanezrouft 039 L3 chondrite (Funk et al. 2011). A troctolitic clast in the Y-794046 (L6) chondrite has an H-chondrite oxygen isotopic composition (Prinz et al. 1984). Wieler et al. (1989) described an L-chondritic inclusion in the Fayetteville H-chondrite regolith breccia, and Fodor and Keil (1975) identified a clast of H-chondrite parentage within the Ngawi LL chondrite. Kakangari chondrite-like fragments were found within the Adrar 003 and Krymka LL3 chondrites (Funk et al. 2011) and exotic fragments in Dhajala (H3) and Krymka (LL3) were described as foreign fine-grained, accretionary objects (Semenenko et al. 2001; Funk et al. 2011). Granitic clasts were found in the LL3-6 ordinary chondrite breccia Adzhi-Bogdo (Bischoff et al. 1993; Sokol et al. 2007; Terada and Bischoff 2009), but their oxygen isotope compositions were similar to those obtained for ordinary chondrites (Sokol et al. 2007b).

In addition, a small CM chondrite clast consisting of olivine crystals and an altered barred olivine chondrule embedded in a matrix of phyllosilicates and sulfide was observed in the Magombedze (H3–5) chondrite (MacPherson et al. 1993). Funk et al. (2011) describe a phyllosilicate- and magnetite-bearing clast having affinities to CI and CM chondrites within the H3 chondrite Sahara 98645. Similarly, a carbonaceous clast was identified in the Dimmitt ordinary chondrite breccia (Rubin et al. 1983), and some further reports on

(possibly) carbonaceous clasts in ordinary chondrites are summarized in Keil (1982).

In summary, the black fragment discovered in Villalbeto de la Peña is a new unique kind of inclusion that can be added to the list of foreign fragments encountered in ordinary chondrites and might bear some similarities to the inclusion described by Brearley et al. (1991). Furthermore, it illustrates the diversity of meteoritic material that was formed, subsequently mixed, and consolidated with other clasts in brecciated chondritic bodies.

Similarities with and Relationship to Winonaites?

In the case of the black fragment within the Villalbeto de la Peña polymict breccia, it remains unclear which kind of foreign clast was incorporated into the host breccia. Mineralogically, this clast does not represent any known meteorite group. Meteorites having such a high abundance of plagioclase besides lunar anorthositic rocks do not exist within our meteorite collections. Anorthosites are magmatic cumulate rocks dominated by plagioclase and are thought to form via crystallization from a (partial) melt. The feldspar-rich composition of the bulk fragment could conceivably represent a portion of such a feldspar-rich cumulate that formed on a differentiated parent body. Partial melting of chondrite precursor material results in the formation of a basaltic melt rich in plagioclase and calcic pyroxene. First melts are anticipated to be rich in feldspar component and incompatible trace elements. The LREE are expected to be afflicted with and enriched in the feldspar which can clearly be seen in Fig. 7 although, the earliest melts from partial melting should also be characterized by very pronounced enrichments in most incompatible elements much higher than what is observed for the plagioclase constituting the dark fragment or rather the bulk fragment itself. Hence, the lower abundances might be more in accordance with plagioclase that crystallized from a basaltic melt and was physically fractionated from pyroxene upon solidification.

Since the oxygen isotopic composition of the black clast is closely related to that of the winonaite Tierra Blanca, this black fragment may be a product of partial melting from the winonaite parent body. As it is known, the Tierra Blanca winonaite has only about 7 vol% plagioclase (e.g., Mittlefehldt et al. 1998) and may have lost significant parts of the plagioclase component during partial melting. However, it should be noted that plagioclase in winonaites is less calcic in composition than plagioclase found in the fragment described here. The bulk REE abundances of the black clast are dominated by a pattern often found for plagioclase from differentiated rocks or plagioclase-dominated lithologies like, e.g., lunar anorthosites. The bulk REE-pattern shows a dominant positive Eu-anomaly and a slight decrease from the LREE (e.g., La approximately $2 \times$ CI) to the HREE (Tb-Lu: $<0.5 \times$ CI), which are close to the detection limits (Fig. 7; Table 3). It is very similar to those of lunar anorthosites (like 60025 in Wiesmann and Hubbard 1975; http://curator.jsc.nasa.gov/lunar/lsc/60025.pdf) and plagioclase from other differentiated meteorites (e.g., eucrites, anomalous eucrites, and winonaites; e.g., Hsu and Crozaz 1996; Floss et al. 2007, 2008). However, REE-patterns of plagioclase are the result of crystal chemical controls and typically show such patterns thus bearing no unequivocal clue to the origin of the fragment.

Thermal History of the Villalbeto de la Peña Meteorite Based on Profiles of Oxygen Isotopes and An-Contents in Plagioclase

Ordinary chondrites experienced prolonged thermal metamorphism on their parent bodies, as evidenced by a broad range of textures and recrystallization fabrics (Sears et al. 1991). Type 6 chondrites, those that underwent the highest degree of metamorphism, experienced peak metamorphic temperatures of 850–950 °C (Huss et al. 2006). Models predict that temperatures in excess of 800 °C could persist as long as approximately 60 Ma in ordinary chondrite parent bodies (Bennett and McSween 1996). These temperatures may also have existed for a shorter length of time at the bottom of asteroidal regolith (Kessel et al. 2007).

A unique opportunity to decipher the conditions of metamorphism on ordinary chondrites is afforded by the exotic feldspar-rich clast in the Villalbeto de la Peña meteorite. The sharp boundary between the host and the black clast, coupled with a recrystallized rim at its interface, suggests that the object was incorporated into the ordinary chondrite parent body prior to metamorphism. Furthermore, the varying plagioclase composition is inconsistent with crystallization of an injected melt. Calcium-rich plagioclase would crystallize first at the boundary with the meteorite host. This would leave a residual, Na-rich interior, opposite to our observations. Dyl et al. (2009, 2012) could show that the zoning profiles in O and of An in plagioclase of the same object cannot be produced under dry metamorphic conditions. The time scales required to produce the compositional zoning in plagioclase are three orders of magnitude greater than those required by oxygen; the entire inclusion would be equilibrated in $^{17,18}O$ in the time required to reproduce the compositional variation (Dyl et al. 2009, 2012). We illustrate in Dyl et al. (2012)

that the geochemical trends observed between the ordinary chondrite host and the Villalbeto black clast are consistent with short-lived hydrothermal alteration on the L chondrite parent body. Both the composition of the plagioclase and the oxygen isotope ratio are modeled using experimental reaction rates and diffusion data, respectively. In both cases, conditions correspond to $T = 800$ °C and $P(H_2O) = 1$ bar. Using these parameters, both the "albitization" of plagioclase and self-diffusion of oxygen in the Villalbeto de la Peña clast correspond to time scales of 1–10 yr of hydrothermal activity on the parent body. Only below 625 °C are time scales in excess of 100 yr required to reproduce both trends. This alteration need not be continuous; the clast could be recording multiple episodes of water-rock reactions. This interpretation would explain the coarse-grained rim observed; it would be the "surface" that controlled the dissolution-reprecipitation reactions between fluid and feldspar.

The occurrence of halite in the metamorphosed chondrites Zag (H3–6) and Monahans (H5) appears to be of asteroidal origin (Zolensky et al. 1999; Rubin et al. 2002), supporting the presence of a brine during high-grade metamorphism of chondrite parent bodies. Rubin et al. (2002) suggested a scenario for the formation in which extensive parent-body processing (metamorphism, breccia formation, regolith gardening) occurred before precipitation of halides from aqueous solutions within porous regions of the asteroid. In the case of the Villalbeto black clast, such aqueous fluids were probably still present during metamorphism after incorporation of the clast into the brecciated parent-body host rock. This could explain the intimate intergrowth and the consolidated integration of the fragment into the rock and thus a blurring of former sharply defined contacts between host rock and incorporated fragment.

Several other studies also suggest that aqueous alteration occurred within the parent bodies of ordinary chondrites. These are summarized by Brearley (2006). Distinct alteration effects were found in the matrices of Semarkona (LL3) and Chainpur (LL3) in the form of phyllosilicates and calcite (Hutchison et al. 1987; Alexander et al. 1989). Hutchison et al. (1987) describe trains of calcites that decorate the margins of chondrules and clasts, indicating formation after accretion as well as alteration veins in the matrix of Semarkona (LL3) that penetrate into chondrules. Also, Grossman et al. (2000) found a radial pyroxene chondrule in Semarkona that underwent early alteration by producing a bleached zone around its exterior. Concerning the very elevated D/H ratios in the matrix of the same chondrite, Deloule and Robert (1995) suggested that this behavior results from the presence of interstellar water.

Time of Aqueous Alteration, Thermal, and Impact Metamorphism

As indicated by the oxygen isotope composition the black inclusion formed on a completely different parent body with a winonaite-like oxygen isotope signature. Certainly, the fragment must have been ejected from this parent body and must have been transported and mixed into the fragmented Villalbeto de la Peña parent-body materials. The metamorphism certainly occurred after the incorporation of the black clast into the host rock and lithification (Kieffer 1975; Bischoff et al. 1983; Bischoff and Stöffler 1992). This is clearly indicated by the recrystallized appearance within the boundary area (Fig. 2b) and by the profiles in oxygen isotopes (Fig. 6) and An-contents in plagioclase (Fig. 4). As described by Dyl et al. (2012) in more detail, the unique geochemical trends recorded in this fragment require the presence of a fluid or volatile phase during subsequent thermal metamorphism. The bulk rock was shocked again after the metamorphism as indicated by shock veins cutting through the black fragment.

Acknowledgments—We thank Ulla Heitmann, Anna Sokol, Thomas Jording, Frank Bartschat, Joachim Krause, and Christian Vollmer (Münster) for sample preparation and technical and analytical support. We thank the reviewers Christine Floss, Alan Rubin, and Alex Ruzicka and the Associate Editor Gretchen Benedix for their fruitful comments and suggestions. This work was partly supported by the German Research Foundation (DFG) within the Priority Program "The First 10 Million Years—A Planetary Materials Approach" (SPP 1385).

Editorial Handling—Dr. Gretchen Benedix

REFERENCES

Alexander C. M. O'D., Hutchison R., and Barber D. J. 1989. Origin of chondrule rims and interchondrule matrices in unequilibrated ordinary chondrites. *Earth and Planetary Science Letters* 95:187–207.

Anders E. and Grevesse N. 1989. Abundances of the elements: Meteoritic and solar. *Geochimica et Cosmochimica Acta* 53:197–214.

Armstrong J. T. 1991. Quantitative elemental analysis of individual microparticles with electron beam instruments. In *Electron probe quantitation*, edited by Heinrich K. F. J. and Newbury D. E. New York: Plenum Press. pp. 261–315.

Bennett M. E. and McSween H. Y. 1996. Revised model calculations for the thermal histories of ordinary chondrite parent bodies. *Meteoritics & Planetary Science* 31:783–792.

Bischoff A. and Keil K. 1983a. Ca-Al-rich chondrules and inclusions in ordinary chondrites. *Nature* 303:588–592.

Bischoff A. and Keil K. 1983b. Catalog of Al-rich chondrules, inclusions and fragments in ordinary chondrites. Special

Publication No. 22. Albuquerque: University of New Mexico, Institute of Meteoritics. pp. 1–33.
Bischoff A. and Keil K. 1984. Al-rich objects in ordinary chondrites: Related origin of carbonaceous and ordinary chondrites and their constituents. *Geochimica et Cosmochimica Acta* 48:693–709.
Bischoff A. and Stöffler D. 1992. Shock metamorphism as a fundamental process in the evolution of planetary bodies: Information from meteorites. *European Journal of Mineralogy* 4:707–755.
Bischoff A., Rubin A. E., Keil K., and Stöffler D. 1983. Lithification of gas-rich chondrite regolith breccias by grain boundary and localized shock melting. *Earth and Planetary Science Letters* 66:1–10.
Bischoff A., Palme H., Spettel B., Clayton R. N., and Mayeda T. K. 1988. The chemical composition of dark inclusions from the Allende meteorite. Proceedings, 19th Lunar and Planetary Science Conference. pp. 88–89.
Bischoff A., Palme H., and Spettel B. 1989. Al–rich chondrules from the Ybbsitz H4–chondrite: Evidence for formation by collision and splashing. *Earth and Planetary Science Letters* 93:170–180.
Bischoff A., Geiger T., Palme H., Spettel B., Schultz L., Scherer P., Schlüter J., and Lkhamsuren J. 1993. Mineraolgy, chemistry, and noble gas contents of Adzhi-Bogdo—An LL3-6 chondritic breccia with L-chondritic and granitoidal clasts. *Meteoritics* 28:570–578.
Bischoff A., Gerel O., Buchwald V. F., Spettel B., Loeken T., Schultz L., Weber H. W., Schlüter J., Baljinnyam L., Borchuluun D., Byambaa C., and Garamjav D. 1996. Meteorites from Mongolia. *Meteoritics & Planetary Science* 31:152–157.
Bischoff A., Scott E. R. D., Metzler K., and Goodrich C. A. 2006. Nature and origins of meteoritic breccias. In *Meteorites and the early solar system II*, edited by Lauretta D. S. and McSween H. Y., Jr. Tucson, Arizona: The University of Arizona Press. pp. 679–712.
Bischoff A., Horstmann M., Pack A., Laubenstein M., and Haberer S. 2010. Asteroid 2008 TC_3—Almahata Sitta: A spectacular breccia containing many different ureilitic and chondritic lithologies. *Meteoritics & Planetary Science* 45:1638–1656.
Bischoff A., Vogel N., and Roszjar J. 2011. The Rumuruti chondrite group—Invited review. *Chemie der Erde—Geochemistry* 71:101–134.
Brearley A. J. 2006. The action of water. In *Meteorites and the early solar system II*, edited by Lauretta D. S. and McSween H. Y., Jr. Tucson, Arizona: The University of Arizona Press. pp. 587–624.
Brearley A. J., Casanova I., Miller M. L., and Keil K. 1991. Mineralogy and possible origin of an unusual Cr-rich inclusion in the Los Martinez (L6) chondrite. *Meteoritics* 26:287–300.
Clayton R. N. and Mayeda T. K. 1996. Oxygen isotope studies of achondrites. *Geochimica et Cosmochimica Acta* 60:1999–2017.
Clayton R. N., Mayeda T. K., Goswami J. N., and Olsen E. J. 1991. Oxygen isotope studies of ordinary chomdrites. *Geochimica et Cosmochimica Acta* 55:2317–2337.
Deloule E. and Robert F. 1995. Interstellar water in meteorites? *Geochimica et Cosmochimica Acta* 59:4695–4706.
Dodd R. T. 1974. Petrology of the St. Mesmin chondrite. *Contributions to Mineralogy and Petrology* 46:129–145.
Dyl K. A., Bischoff A., Ziegler K., Wimmer K., and Young E. D. 2009. Evidence for aqueous alteration in ordinary chondrites from compositional and oxygen isotopic trends in an exotic fragment. *Meteoritics & Planetary Science* 44:A65.
Dyl K. A., Bischoff A., Ziegler K., Wimmer K., and Young E. D. 2009. Metamorphic conditions within the Villalbeto de la Peña L-chondrite parent body based on petrologic and UV laser fluorination oxygen isotopic studies on an unique fragment (abstract #2506). 40th Lunar and Planetary Science Conference. CD-ROM.
Dyl K. A., Bischoff A., Ziegler K., Young E. D., Wimmer K., and Bland P. A. 2012. Early solar system hydrothermal activity in chondritic asteroids on 1–10-year timescales. *Proceedings of the National Academy of Sciences* 109:18306–18311.
Endreß M., Keil K., Bischoff A., Spettel B., Clayton R. N., and Mayeda T. K. 1994. Origin of dark clasts in the Acfer 059/El Djouf 001 CR2 chondrite. *Meteoritics* 29:26–40.
Floss C., Jolliff B. L., Benedix G. K., Stadermann F. J., and Reid J. 2007. Hammadah al Hamra 193: The first amphibole-bearing winonaite. *American Mineralogist* 92: 460–467.
Floss C., Crozaz G., Jolliff B., Benedix G., and Colton S. 2008. Evolution of the winonaite parent body: Clues from silicate mineral trace element distributions. *Meteoritics & Planetary Science* 43:657–674.
Fodor R. V. and Keil K. 1975. Implications of poikilitic textures in LL-group chondrites. *Meteoritics* 10:325–340.
Fodor R. V. and Keil K. 1978. Catalog of lithic fragments in LL-Group chondrites. Special Publication No. 19. Albuquerque: University of New Mexico, Institute of Meteoritics. 38 p.
Fruland R. M., King E. A., and McKay D. S. 1978. Allende dark inclusions. Proceedings, 9th Lunar and Planetary Science Conference. pp. 1505–1329.
Funk C., Bischoff A., and Schlüter J. 2011. Xenoliths in carbonaceous and ordinary chondrites. *Meteoritics & Planetary Science* 46:A71.
Gomes C. B. and Keil K. 1980. *Brazilian stone meteorites*. Albuquerque: University of New Mexico Press. 161 p.
Grossman J. N., Alexander C. M. O'D., Wang J. H., and Brearley A. J. 2000. Bleached chondrules: Evidence for widespread aqueous processes on the parent asteroids of ordinary chondrites. *Meteoritics & Planetary Science* 35:467–486.
Horstmann M., Bischoff A., Pack A., Albrecht N., Weyrauch M., Hain H., Roggon L., and Schneider K. 2012. Mineralogy and oxygen isotope composition of new samples from the Almahata Sitta strewn field (abstract #5052). *Meteoritics & Planetary Science* 47:A193.
Hsu W. and Crozaz G. 1996. Mineral chemistry and the petrogenesis of eucrites: I. Noncumulate eucrites. *Geochimica et Cosmochimica Acta* 60:4571–4591.
Huss G. R., Rubin A. E., and Grossman J. N. 2006. Thermal metamorphism in chondrites. In *Meteorites and the early solar system II*, edited by Lauretta D. S. and McSween H. Y., Jr. Tucson, Arizona: The University of Arizona Press. pp. 567–586.
Hutchison R., Alexander C. M. O'D., and Barber D. J. 1987. The Semarkona meteorite: First recorded occurrence of smectite in an ordinary chondrite, and its implications. *Geochimica et Cosmochimica Acta* 51:1875–1882.
Keil K. 1982. Composition and origin of chondritic breccias. In *Workshop on lunar breccias and soils and their meteoritic analogs*, edited by Taylor G. J. and Wilkening L. L. LPI

Technical Report 82-02. Houston, Texas: Lunar Planetary Institute. pp. 65–83.
Kessel R., Beckett J. R., and Stolper E. M. 2007. The thermal history of equilibrated ordinary chondrites and the relationship between textural maturity and temperature. *Geochimica et Cosmochimica Acta* 71:1855–1881.
Kieffer S. W. 1975. From regolith to rock by shock. *The Moon* 13:301–320.
Krot A., Ivanova M. A., and Wasson J. T. 1993. The origin of chromitic chondrules and the volatility of Cr under a range of nebular conditions. *Earth Planetary Science Letters* 119:569–584.
Llorca J., Trigo-Rodríguez J. M., Ortiz J. L., Docobo J. A., Garcia-Guinea J., Castro-Tirado A. J., Rubin A. E., Eugster O., Edwards W., Laubenstein M., and Casanova I. 2005. The Villalbeto de la Peña meteorite fall: I. Fireball energy, meteorite recovery, strewn field, and petrography. *Meteoritics & Planetary Science* 40:795–804.
MacPherson G. J., Jarosewich E., and Lowenstein P. 1993. Magombedze: A new H-chondrite with light-dark structure. *Meteoritics* 28:138–142.
Mittlefehldt D. W., McCoy T. J., Goodrich C. A., and Kracher A. 1998. Non-chondritic meteorites from asteroidal bodies. In *Planetary materials*, edited by Papike J. J. Reviews in Mineralogy, vol. 36. Washington, D.C.: Mineralogical Society of America. pp. 4-1–4-195.
Prinz M., Nehru C. E., Weisberg M. K., Delany J. S., Yanai K., and Kojima H. 1984. H-chondritic clasts in a Yamato L6 chondrite: Implications for metamorphism. *Meteoritics* 19:292–293.
Rubin A. E. 1990. Kamacite and olivine in ordinary chondrites: Intergroup and intragroup relationships. *Geochimica et Cosmochimica Acta* 54:1217–1232.
Rubin A. E. and Bottke W. F. 2009. On the origin of shocked and unshocked CM clasts in H-chondrite regolith breccias. *Meteoritics & Planetary Science* 44:701–724.
Rubin A. E., Rehfeldt A., Peterson E., Keil K., and Jarosewich E. 1983. Fragmental breccias and the collisional evolution of ordinary chondrite parent bodies. *Meteoritics* 18:179–196.
Rubin A. E., Zolensky M. E., and Bodnar R. J. 2002. The halite-bearing Zag and Monahans (1998) meteorite breccias: Shock metamorphism, thermal metamorphism and aqueous alteration on the H-chondrite parent body. *Meteoritics & Planetary Science* 37:125–141.
Russell S. S., Folco L., Grady M. M., Zolensky M. E., Jones R., Righter K., Zipfel J., and Grossman J. N. 2004. The Meteoritical Bulletin, No. 88. *Meteoritics & Planetary Science* 39:A215–A272.
van Schmus W. R. and Ribbe P. H. 1968. The composition and structural state of feldspar from chondritic meteorites. *Geochimica et Cosmochimica Acta* 32:1327–1342.
Sears D. W. G., Hasan E. A., Batchelor J. D., and Lu J. 1991. Chemical and physical studies of type 3 chondrites—XI: Metamorphism, pairing, and brecciation of ordinary chondrites. Proceedings, 21st Lunar and Planetary Science Conference. pp. 493–512.
Semenenko V. P., Bischoff A., Weber I., Perron C., and Girich A. L. 2001. Mineralogy of fine-grained material in the Krymka (LL3.1) chondrite. *Meteoritics & Planetary Science* 36:1067–1085.
Sharp Z. D. 1990. A laser-based microanalytical method for the in situ determination of oxygen isotope ratios of silicates and oxides. *Geochimica et Cosmochimica Acta* 54:1353–1357.
Sokol A. K., Bischoff A., Marhas K. K., Mezger K., and Zinner E. 2007a. Late accretion and lithification of chondritic parent bodies: Mg isotope studies on fragments from primitive chondrites and chondritic breccias. *Meteoritics & Planetary Science* 42:1291–1308.
Sokol A. K., Chaussidon M., Bischoff A., and Mezger K. 2007b. Occurrence and origin of igneous fragments in chondritic breccias. *Geochimica et Cosmochimica Acta* 71 (Suppl. 1):A952.
Stöffler D., Ostertag R., Jammes C., Pfannschmidt G., Sen Gupta P. R., Simon S. B., Papike J. J., and Beauchamp R. H. 1986. Shock metamorphism and petrography of the Shergotty achondrite. *Geochimica et Cosmochimica Acta* 50:889–903.
Stöffler D., Keil D., and Scott E. R. D. 1991. Shock metamorphism of ordinary chondrites. *Geochimica et Cosmochimica Acta* 55:3845–3867.
Terada K. and Bischoff A. 2009. Asteroidal granite-like magmatism 4.53 Gyr ago. *The Astrophysical Journal* 699: L68–L71.
Trigo-Rodríguez J. M., Borovicka J., Spurny P., Ortiz J. L., Docobo J. A., Castro-Tirado A. J., and Llorca J. 2006. The Villalbeto de la Peña meteorite fall: II. Determination of the atmospheric trajectory and orbit. *Meteoritics & Planetary Science* 41:505–517.
Wieler R., Graf T., Pedroni A., Signer P., Pellas P., Fieni C., Suter M., Vogt S., Clayton R. N., and Laul J. C. 1989. Exposure history of the regolithic chondrite Fayetteville: II. Solar-gas-free light inclusions. *Geochimica et Cosmochimica Acta* 53:1449–1459.
Wiesmann H. and Hubbard N. J. 1975. A compilation of the lunar sample data generated by the Gast, Nyquist and Hubbard lunar sample PI-ships. JSC. http://curator.jsc.nasa.gov/lunar/lsc/60025.pdf
Wilkinson S. L. and Robinson M. S. 2000. Bulk density of ordinary chondrite meteorites and implications for asteroidal internal structure. *Meteoritics & Planetary Science* 35:1203–1213.
Young E. D., Coutts D. W., and Kapitan D. 1998a. UV laser ablation and irm-GCMS microanalysis of O-18/O-16 and O-17/O-16 with application to a calcium-aluminium-rich inclusion from the Allende meteorite. *Geochimica et Cosmochimica Acta* 62:3161–3168.
Young E. D., Nagahara H., Mysen B. O., and Audet D. M. 1998b. Non-Rayleigh oxygen isotope fractionation by mineral evaporation: Theory and experiments in the system SiO_2. *Geochimica et Cosmochimica Acta* 62:3109–3116.
Zolensky M. and Ivanov A. 2003. The Kaidun microbreccia meteorite: A harvest from the inner and outer asteroid belt. *Chemie der Erde* 63:185–246.
Zolensky M. E., Bodnar R. J., Gibson E. K., Jr., Nyquist L. E., Resse Y., Shih C.-T., and Wiesman H. 1999. Asteroidal water within fluid inclusion-bearing halite in an H5 chondrite, Monahans. *Science* 285:1377–1379.